*Korean J. Chem. Eng.*, 32(4), 753-760 (2015)
DOI: 10.1007/s11814-014-0261-6

pISSN: 0256-1115
eISSN: 1975-7220

# Study on the thin film composite poly(piperazine-amide) nanofiltration membranes made of different polymeric substrates: Effect of operating conditions

**Nurasyikin Misdan*,**, Woei Jye Lau*,**, Chi Siang Ong*,**, Ahmad Fauzi Ismail*,†, and Takeshi Matsuura*,***

*Advanced Membrane Technology Research Centre (AMTEC), Universiti Teknologi Malaysia, 81310 Skudai, Johor, Malaysia
**Faculty of Petroleum and Renewable Energy Engineering, Universiti Teknologi Malaysia, 81310 Skudai, Johor, Malaysia
***Department of Chemical and Biological Engineering, Industrial Membrane Research Institute,
University of Ottawa, 161 Louis Pasteur St., Ottawa, ON KIN 6N5, Canada
(*Received 16 June 2014 • accepted 1 September 2014*)

**Abstract**−Three composite nanofiltration (NF) membranes made of different substrate materials--polysulfone (PSf), polyethersulfone (PES) and polyetherimide (PEI)--were successfully prepared by interfacial polymerization technique. Prior to filtration tests, the composite NF membranes were characterized using field emission scanning electron microscope (FESEM), atomic force microscope (AFM) and X-ray photoelectron spectroscope (XPS). It was observed that the surface properties of composite NF membranes were obviously altered with the use of different substrate materials. The separation performance of the prepared composite NF membranes was further evaluated by varying operating conditions, which included feed salt concentration and operating temperature. Experimental results showed that the water flux of all TFC membranes tended to decrease with increasing $Na_2SO_4$ concentration in feed solution, due to the increase in feed osmotic pressure. Of the three TFC membranes studied, PSf-based membrane demonstrated the highest salt rejection but lowest water flux owing to its highest degree of polyamide cross-linking as shown in XPS data. With respect to thermal stability, PEI-based TFC membrane outperformed the rest, overcoming the trade-off effect between permeability and rejection when the feed solution temperature was gradually increased from 30 °C to 80 °C. In addition, the relatively smoother surface of hydrophilic PEI-based membrane when compared with PSf-based membrane was found to be less susceptible to BSA foulants, leading to lower flux decline. This is because smoother surface of polyamide layer would have minimum "valley clogging," which improves membrane anti-fouling resistance.

Keywords: Poly(piperazine-amide), Thin Film Composite, Interfacial Polymerization, Nanofiltration

## INTRODUCTION

Nanofiltration (NF), a process that lies between ultrafiltration and reverse osmosis, has emerged as an important and fast-growing separation technology in water treatment and purification processes. Compared to typical asymmetric NF membrane, thin film composite (TFC) NF membrane, which consists of a very thin polyamide (PA) active layer, enables to separate small solutes (200-1,000 $g \cdot mol^{-1}$) from water at a very promising water permeability [1,2]. Industrially, the applications of TFC NF membranes appear mainly in waste water treatment, water softening, dyes and heavy metals removal, food and pharmaceutical processes, seawater desalination and organic solvent separation [2-9].

For certain industrial applications, separation processes require relatively high temperature (around 70-90 °C) to operate and, thermally stable polymeric membranes are therefore highly desired [10, 11]. For TFC NF membrane, its thermal stability is not only dependent on the top PA selective layer but also the bottom substrate layer. To date, polysulfone (PSf) is still the most commonly used polymer in preparing the substrate of the TFC membranes, mainly due to its relatively good mechanical, chemical and thermal stability as well as sustainability against bacterial attack compared to other polymer-based substrates [10,12,13]. However, the relatively low glass transition temperature ($T_g$) and low maximum allowable operating temperature (<50 °C) for PSf-based TFC membrane [14] might limit its wide industrial applications. Therefore, numerous efforts have been devoted to explore the potential of other polymeric materials that can be used to replace PSf in the preparation of TFC membrane substrate. These include polyvinylidene fluoride (PVDF) [15], polypropylene (PP) [16], polyetherimide (PEI) [17,18] and poly (phthalazinone ether sulfone ketone) (PPESK) [19].

To study the performance of TFC membrane made of new type of substrate material, Han et al. [20] in the year 2011 prepared a composite membrane using copoly(phthalazinonebiphenyl ether sulfone) (PPBES) as the substrate material. The membrane flux was reported to increase tremendously with a slight reduction in the salt rejection when the operation temperature was increased up to 85 °C at 1.0 MPa. One year later, poly(phthalazione ether nitrile ketone) (PPENK) was introduced by Hu et al. [11], as membrane substrate to prepare thermally stable composite NF membrane. It was reported that the resultant polyamide/PPENK composite membrane could display up to four-times increment of permeation flux without significant change of salt rejection when the temperature of feed solution was increased from 20 °C to 80 °C at operating pressure of 1.0 MPa. Based on these findings, it can be said that substrate membrane makes an important contribution not only to

†To whom correspondence should be addressed.
E-mail: afauzi@utm.my, fauzi.ismail@gmail.com

**Table 1. Properties of the substrate membranes**

| Substrate material | Organic structure | Glass transition temperature ($T_g$) |
|---|---|---|
| Polysufone (PSf) | 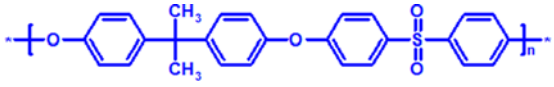 | 185 °C[a] |
| Polyethersulfone (PES) | 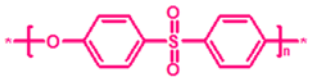 | 220 °C[a] |
| Polyetherimide (PEI) | 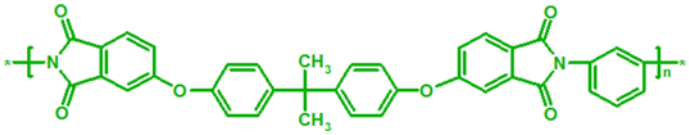 | 217 °C[b] |

**adapted from* [a]Solvayplastics; [b]Sabic

the variation in PA properties but also to the performance of composite performance, particularly at relatively high operating temperature.

In view of the importance of polymeric substrate on membrane performance, our main objective was to study the effect of three different substrate properties, polysulfone (PSf), polyethersulfone (PES) and polyetherimide (PEI), on the formation of poly(piperazine-amide) layer and further its separation performance at different operating conditions, which include variation in feed concentration and operating temperature. Table 1 presents the properties of these three polymeric materials with respect to $T_g$ together with their respective organic structure. In addition to the separation performance tests, the anti-fouling property of the prepared composite NF membranes against bovine serum albumin (BSA) was also investigated. It is because the membrane with low anti-fouling resistance tends to have severe foulant deposition on membrane top surface and/or within membrane pore, which as a consequence, might deteriorate membrane performance and shorten its lifespan [12,21].

## EXPERIMENTAL

### 1. Materials

Both polysulfone (Udel® P-1700) and polyethersulfone were purchased from Solvay Specialty Polymers, USA. Polyetherimide (ULTEM) was supplied from Sabic, Singapore. These three polymers were later used to fabricate substrates for TFC membranes. Polyvinylpyrrolidone (PVP) K30 of $M_w$ 40,000 g·mol$^{-1}$ purchased from FlukaChemie GmbH, Switzerland was used as the pore forming agent. Trimethylchloride (TMC) and piperazine (PIP) purchased from Sigma Aldrich and Merck, respectively were used to synthesize in-situ PA layer on each substrate made of PSf, PES and PEI. 1-methyl-2-pyrrolidone (Purity>99.5%) and cyclohexane supplied from Merck were used as solvent without further purification. $Na_2SO_4$ supplied by GCE Laboratory Chemicals was used to prepare aqueous salt solution for membrane flux and rejection measurement. Bovine serum albumin (BSA) (67 kDa) supplied from Sigma Aldrich was used as model foulant to study membrane anti-fouling property.

### 2. TFC Membrane Reparation

2-1. Preparation of Microporous Substrate

Asymmetric PSf substrate was prepared via phase inversion technique using a polymer dope comprised of 15 wt% polymer. To increase the porosity of the substrate prepared, 1 wt% PVP K30 was added into the casting dope as a pore forming agent. PVP was first dissolved in NMP solvent, followed by the addition of PSf. The mixture was stirred continuously until a homogeneous polymeric solution was obtained. The solution was then cast on a glass plate using a casting bar to a thickness of approximately 100 μm. The cast polymer solution film was kept for 30 s at ambient temperature before being immersed into a water coagulation bath (ambient temperature) together with the glass plate. The membrane peeled off from the glass plate was then washed thoroughly with de-ionized water to remove residual solvent and kept wet at 5 °C prior to use. PES and PEI substrates were also prepared under the same conditions as PSf. Those membranes are denoted as PSf, PES and PEI substrate, respectively.

2-2. Preparation of Polyamide Thin Active Layer

TFC NF membranes made of different substrates were prepared via *in-situ* interfacial polymerization of PIP and TMC. The substrate was initially taped onto the glass plate followed by immersion in an aqueous solution of 2% (w/v) PIP for 120 s. The excess solution at the impregnated membrane surface was removed using a soft rubber roller. It was followed by immersion of substrate into cyclohexane solution of 0.15% (w/v) TMC for 10 s, which resulted in *in-situ* formation of an ultra-thin PA layer over the microporous substrate. Subsequently, the resulting composite membrane was cured at 80 °C for 180 s followed by thorough rinsing with de-ionized water. Finally, the composite membrane was stored in de-ionized water at 5 °C prior to use. The TFC NF membranes so prepared were denoted as PSf-based TFC, PES-based TFC and PEI-based TFC, depending on the substrate used to make the composite membrane.

2-3. TFC NF Membrane Performance Evaluation

The flux and rejection of the fabricated TFC NF membranes were studied using a dead-end filtration system (Sterlitech™ HP4750 Stirred Cell) to which feed pressure was supplied from a pressurized nitrogen cylinder. TFC membranes were initially compacted at a pressure of 0.8 MPa with DI water for about 1 h before starting any measurement. The NF experiments were then performed using 1,000 ppm $Na_2SO_4$ solution at operating pressure and temperature set at 0.6 MPa and 25 °C, respectively. Membrane water flux (F) was subsequently calculated with the following equation:

$$F = \frac{V}{t \times A} \quad (1)$$

where V is the permeate volume (L), A is the membrane area ($m^2$) and t is the time to obtain V (h).

A bench conductivity meter (Jenway 4520) was used to measure the salt concentration in the feed and permeate solutions. The membrane salt rejection, R (%) was then determined with the following equation:

$$R = \left(1 - \frac{C_p}{C_f}\right) \times 100 \quad (2)$$

where $C_p$ is the permeate concentration (ppm) and $C_f$ is the feed concentration (ppm), respectively. To study the effect of operating conditions on the performances of three resultant TFC NF membranes, feed salt concentration and temperature were varied in the range of 1,000-3,000 ppm and 30-80 °C, respectively.

2-4. Membrane Biofouling Experiment

Biofouling experiments were conducted by subjecting the TFC NF membrane to a filtration process of 500 ppm bovine serum albumin (BSA). The operating pressure and temperature were fixed at 0.6 MPa and 25 °C for all the TFC NF membranes. In addition to the permeate flux determination (Eq. (1)), normalized flux (Final flux, $J_f$/Initial flux, $J_o$) was used to evaluate membrane anti-fouling property. The BSA rejection (R) was determined by using the following equation:

$$R(\%) = \left(1 - \frac{C_p}{C_f}\right) \times 100 \quad (3)$$

where $C_p$ and $C_f$ are the BSA concentration (ppm) of permeate and feed solutions, respectively, and are measured by UV-Vis spectrophotometer (DR5000, Hach).

2-5. Substrate and Polyamide Layer Characterization

X-ray photoelectron spectroscopy (XPS, Kratos Axis HS X-ray photoelectron spectrometer, Manchester, UK) analysis was performed to measure the surface elemental composition by using monochromatized Al $K_\alpha$ X-radiation source. Each membrane coupon was cut into the sample pieces of approximately 1 cm. The TFC membrane surfaces were analyzed for specific element content at take-off angle of 45° which corresponded to the X-ray penetration depth of 4.45 nm. Atomic force microscope (AFM) (Multimode 8 AFM instrument equipped with a NanoScope V controller) was used to characterize the surface morphology of the TFC membranes in terms of the roughness parameters. The scanning area of each membrane was 5 μm×5 μm. The top surface morphology of the TFC and substrate membranes was visualized using field emission scanning electron microscope (FESEM) (JEOL JSM-6700F). The contact angle of substrate and polyamide layer was measured using a Phoenix 300 contact angle goniometer (S.E.O. Co., Ltd, Korea). At least ten measurements were made at different locations of a membrane sample and the average value was reported.

## THEORETICAL BACKGROUND

### 1. Irreversible Thermodynamic Model

The ionic transport phenomena through the composite membrane can be described by an irreversible thermodynamic model. In general, the solute flux was influenced by either diffusion or convection which depends on the operating conditions [22,23]. The simplified Spiegler-Kedem-Kachalsky (SKK) model transport equations can be written as follows [22-25]:

$$J_v = L_p(\Delta P - \Delta\pi) \quad (4)$$

$$J_s = P_s(C_m - C_p) + (1-\sigma)J_v \quad (5)$$

where $J_v$ and $J_s$ are, respectively, the solvent flux and the solute flux; $\Delta P$ is the pressure drop; $\Delta\pi$ is the osmotic pressure difference across the membrane; $C_m$ and $C_p$ are, respectively, the solute concentrations at the membrane surface and in the permeate; $P_s$ is the solute permeability; $L_p$ is the permeability of water; and $\sigma$ is the reflection coefficient with $0 \le \sigma \le 1$.

For a pressure-driven NF process, the solute transport through the membrane can be described as the sum of a diffusive and convective flux. Convection solute transport is due to the applied pressure gradient across the membrane, while diffusive transport is caused by the concentration difference across the membrane [23,26]. The observed rejection, $R_{obs}$ can be expressed by the SKK model as follows:

$$R_{obs} = \frac{\sigma\left(1 - \exp\left(-\frac{1-\sigma}{P_S}J_v\right)\right)}{1 - \sigma\exp\left(-\frac{1-\sigma}{P_S}J_v\right)} \quad (6)$$

where $J_v$ is the water flux and $P_s$ is the solute permeability toward the membrane.

From Eq. (6), it is assumed that the observed rejection increases with increasing water flux and achieving a limiting value of $\sigma$ at an infinitely high water flux. For a membrane with high solute rejection, the solute transport is mainly due to the diffusive flow and the convective solute transport is mostly hindered [14,23]. The solute retention may, however, be lower than 100% as solute molecules transport may take place not only by the diffusion but also by the combined solution and diffusion [23].

### 2. Solution-diffusion Model

According to the Solution-diffusion model, water permeability $P_w$ and salt permeability $P_s$ can be described as follows [27-29]:

$$P_w = S_w D_w \quad (7)$$

$$P_s = S_s D_s \quad (8)$$

where $S_w$ and $D_w$ are water solubility and water diffusivity, respectively, while $S_s$ and $D_s$ are salt solubility and salt diffusivity in the polymer, respectively.

The temperature dependence on solute diffusion obeys a relationship similar to the Arrhenius equation, as transport of solute molecules through a membrane is considered a thermally activated process. Thus, the temperature dependence of diffusion is expressed as [30]:

$$D_s = D_0 \cdot \exp\left(\frac{E_D}{R.T}\right) \quad (9)$$

where $D_0$ is the pre exponential factor ($m^2$/s), $E_D$ is the activation energy of diffusion (J/mol), R is the gas constant (8.314J/mol·K) and T is the absolute temperature (K). The activation energy is considered as the energy required to create a gap between polymer

segments in which the solute molecules can diffuse. The temperature dependence of the solubility coefficient $S_s$ on the other hand can be written as:

$$S_s = S_0 \cdot \exp\left(-\frac{\Delta H_s}{R.T}\right) \quad (10)$$

where $S_0$ and $\Delta H_s$ are the pre exponential factor (mol/m$^3$ Pa) and the enthalpy of solution (J/mol), respectively. By substituting Eq. (9) and (10) into Eq. (8), the temperature difference of $P_s$ can be written as follows:

$$P_S = D_0 S_0 \cdot \exp\left(-\frac{E_p}{R.T}\right) \quad (11)$$

where $E_p$ is the activation energy of permeation (i.e., sum of $E_D$ and $\Delta H_s$). In general, permeability increases with increasing temperature.

## RESULTS AND DISCUSSION

### 1. Characteristics of TFC NF Membranes

Fig. 1 shows the FESEM surface images of both composite poly (piperazineamide) NF membranes and substrate membranes. The composite poly(piperazineamide) layer at the top surface of the three TFC membranes is featured by a rough and dense structure with many granules, which is common for many TFC membranes fabricated by *in-situ* polymerization. In contrast to the microporous substrates, visible open pores (of different sizes) can be clearly seen throughout the substrates surface. Note that the poly(piperazineamide) layer, which appeared as ridge-and-valley structure on the top surface of TFC membrane, could be formed regardless of substrate pore size.

The surface AFM image of the prepared TFC membranes is shown in Fig. 2, together with the $R_q$ value. The results show that the roughness value decreases in the following order: PSf-based TFC (21.0 nm)>PEI-based TFC (14.4 nm)>PES-based TFC (12.6 nm). To analyze the surface elemental composition of the prepared TFC membranes, XPS characterization was also performed. Table 2 summarizes the elemental composition (%) of the three prepared TFC membranes with respect to carbon (C), oxygen (O), and nitrogen (N). Theoretically, three different types of PA structures are possibly synthesized over the substrate surface:

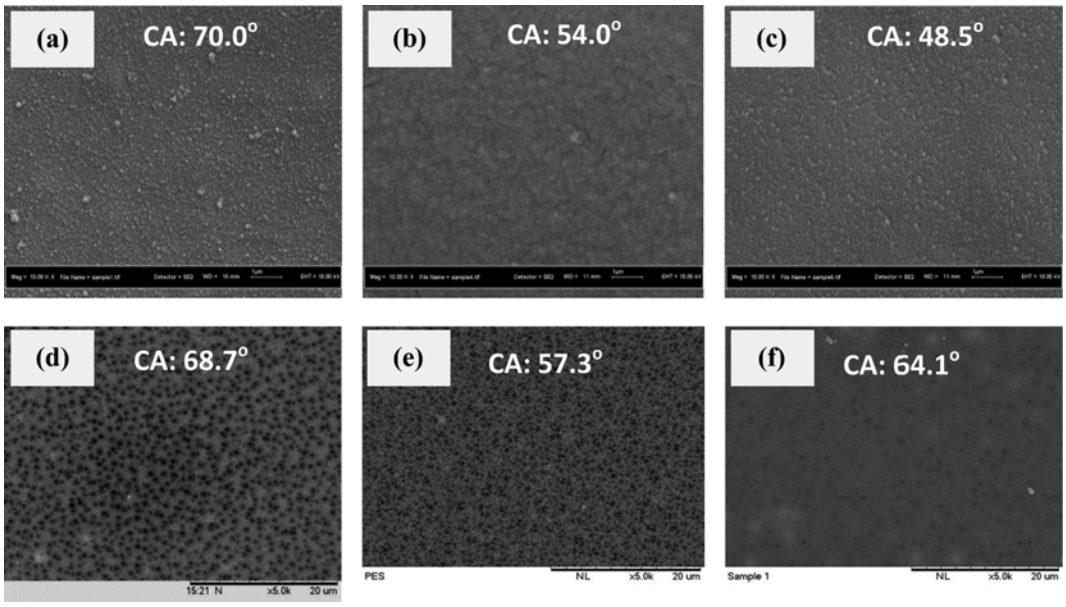


**Fig. 1. Top surface FESEM images of, (a) PSf-based TFC, (b) PES-based TFC, (c) PEI-based TFC, (d) PSf substrate, (e) PES substrate, and (f) PEI substrate together with water contact angle (CA).**

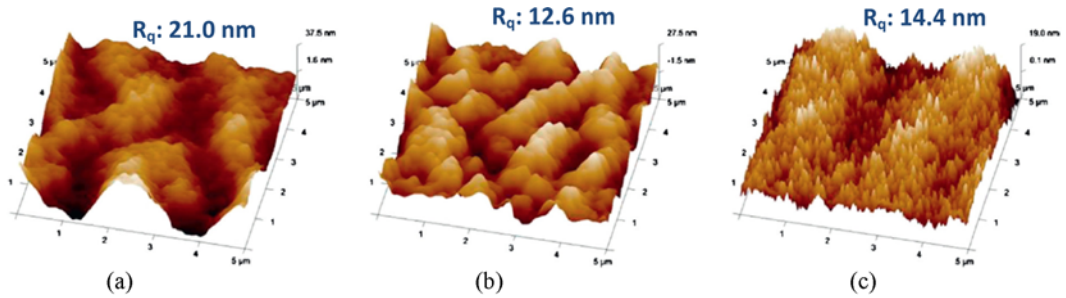


**Fig. 2. AFM images of TFC NF membranes together with $R_q$ surface roughness values, (a) PSf-based TFC, (b) PES-based TFC and (c) PEI-based TFC.**

**Table 2. XPS analysis of TFC NF membranes made over different polymer substrates**

| Membrane | C (%) | O (%) | N (%) | O/N | N/C | O/C |
|---|---|---|---|---|---|---|
| PSf-based TFC (from XPS) | 76.96 | 13.42 | 9.62 | 1.39 | 0.13 | 0.17 |
| PES-based TFC (from XPS) | 79.07 | 15.18 | 5.75 | 2.64 | 0.07 | 0.19 |
| PEI-based TFC (from XPS) | 72.36 | 19.28 | 8.37 | 2.3 | 0.12 | 0.26 |
| **Theoretical values** | | | | | | |
| Totally cross-linking structure | 71.42 | 14.29 | 14.29 | 1.00 | 0.2 | 0.2 |
| Linear structure with a pendant -COOH group | 68.42 | 21.05 | 10.53 | 2.00 | 0.15 | 0.31 |
| Linear structure with two pendant -COOH groups | 65 | 25 | 10 | 2.5 | 0.15 | 0.38 |

(a) total cross-linking: when all the pendant -COCl groups of TMC are involved in cross-linking,

(b) linear structure with a pendant -COOH group: when one pendant -COCl group of TMC is left free without cross-linking and

(c) linear structure with two pendant -COOH groups: when two of pendant -COCl groups are left free.

The last case shows the effect of end-capping of polymerization by TMC. The calculation was made for an extreme case of a PIP-TMC dimer. All the uncross-linked PIP-TMC polymers will display values between the cases of (b) and (c) and the values approach (b) as the chain length of the polymer increases. According to the XPS data, O/N ratio is more reliable and accurate for analysis compared to O/C and N/C ratios as the latter two elemental ratios are likely to be influenced by the C element, which presents in large quantity in polyamide layer, causing the result interpretation rather difficult. Therefore, by comparing the O/N ratio of the membrane obtained from XPS with theoretical values, it can be said that the PSf-based TFC membrane is more like a cross-linking structure, while PES-based and PEI-based TFC membranes are more like linear structures. The in-depth discussion on how the changes in substrate properties, e.g. pore size, porosity, hydrophilicity, and roughness, on the physicochemical properties TFC membrane can be found in our earlier publication [31].

## 2. Performance of TFC NF Membranes

### 2-1. Effect of Salt Concentration

The effect of $Na_2SO_4$ salt concentration on the permeate flux and rejection for the three prepared TFC membranes is shown in Figs. 3 and 4, respectively. The water flux of all the TFC membranes tends to decrease with increasing $Na_2SO_4$ concentration from 1,000 to 3,000 ppm. The decrease in flux can be mainly attributed to the increase in osmotic pressure which results from the increase in salt concentration used in the feed [32,33]. As for the salt rejection, the separation efficiency of PSf-based and PES-based TFC membranes was found to decrease with the salt concentration in which PSf-based membrane displays more obvious drop in salt rejection compared to PES-based membrane. The rejection of PSf-based membrane is reported to fall in the range of 95.7-97.1% in comparison to 93.5-94.5% reported in PES-based membrane. PEI-based membrane on the other hand shows a very stable salt rejection (aver-

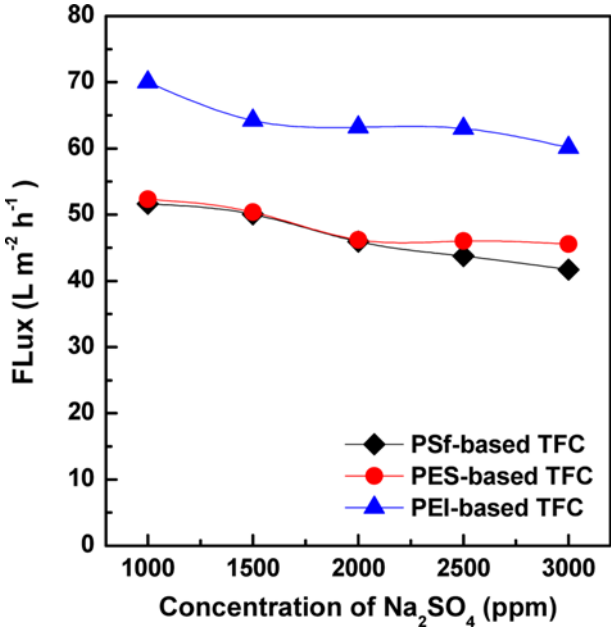


**Fig. 3. Water permeability of TFC NF membranes at various $Na_2SO_4$ concentrations.**

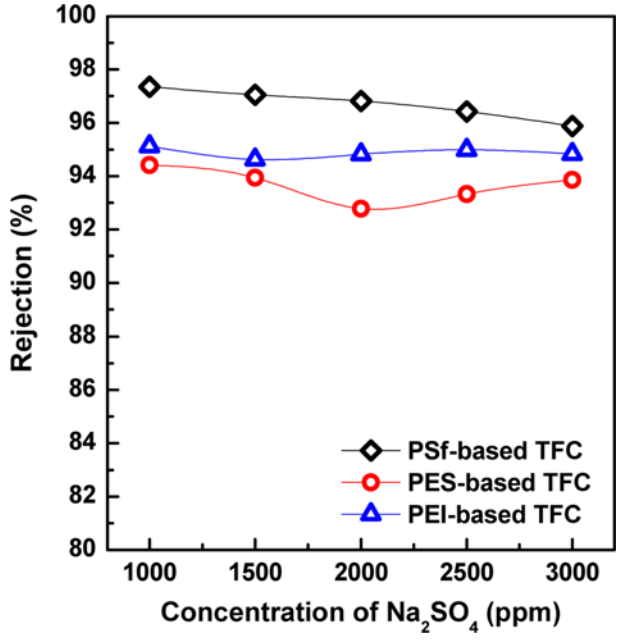


**Fig. 4. Salt rejection of TFC NF membranes at various $Na_2SO_4$ concentrations.**

age 95%) within the range of salt concentration studied. In general, the Donnan effect plays a significant role in TFC polyamide membrane in retaining salt from passing through membrane structure. When the concentration of feed solution is increased, the dissolved salts play an important role in damping out electrostatic repulsion, causing electrolyte retention of charged membrane to decrease and further reduce membrane efficiency in retaining salt [34]. However, the relatively stable performance of PEI-based membrane in retaining salt solute of low range concentration might be due to its higher surface charge density compared to the PSf- and PES-based membrane. Furthermore, the highest water flux shown by PEI-based membrane could be due to its comparatively linear structure of polyamide layer coupled with the highest degree of hydrophilicity (i.e., lowest contact angle).

2-2. Effect of Feed Solution Temperature

The thermal stability of TFC membranes is usually studied within a range of operation temperature from 30 °C to 80 °C. It is generally known that temperature has significant effects on both flux and salt separation of the composite membrane, as polymer molecular chain tends to become more flexible and easier to deform at high operating temperature [35,36].

Fig. 5 shows the experimentally obtained flux of each TFC NF membrane, which is determined at different operating temperature in the range of 30-80 °C. As can be seen, the membrane flux increases with the temperature in which the PEI-based membrane shows the highest flux enhancement followed by PSf- and PES-based membrane. With respect to salt rejection as shown in Fig. 6, the salt rejection of PSf-based membrane decreases greatly from around 96.5% to 91% with increasing operating temperature from 30 to 80 °C. The deterioration of salt rejection at high operating temperature is very common for TFC membrane made of PSf substrate, and that is why this kind of membrane substrate is not recommended for applications which require operating temperature

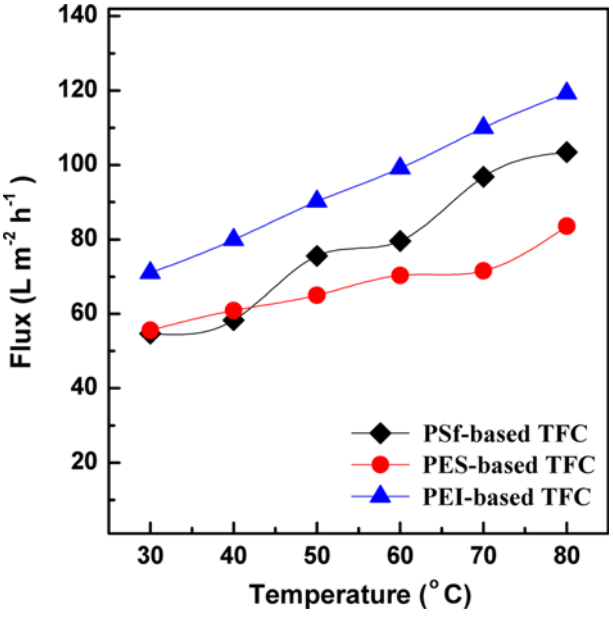


**Fig. 5. Water permeability of TFC NF membranes as a function of operating temperature.**

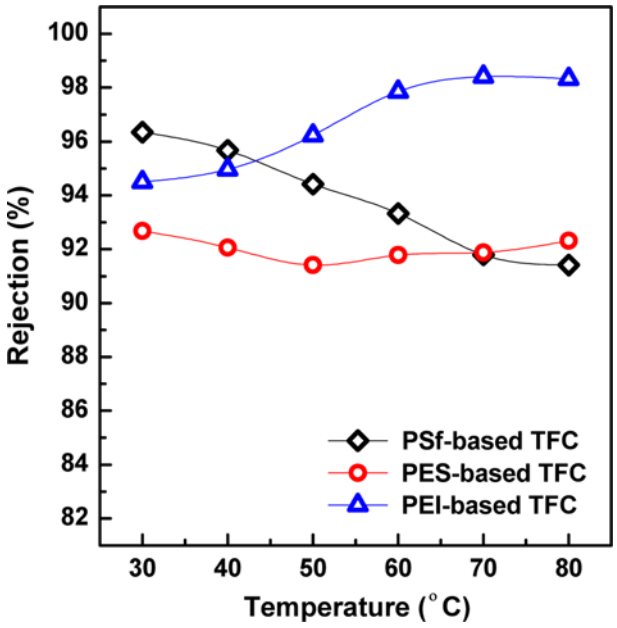


**Fig. 6. Salt rejection of TFC NF membranes as a function of operating temperature.**

>50 °C. Interestingly, the salt separation efficiency of PEI-based membrane is not negatively affected by the high operating temperature. The rejection instead increases gradually from 94.5 to 98% with increasing temperature from 30 to 80 °C. The performance of the PES-based membrane, however, does not change much within the studied temperature range. Its rejection remains at between 91 and 93% irrespective of operating temperature. Applying the Arrhenius plot for the salt passage, the activation energies of salt passage are 16.23, 0.78 and −25.39 kJ/mol, respectively, for PSf-, PES- and PEI-based TFC membranes. A remarkable change in the activation energy is observed by employing different polymeric substrates for TFC membrane in which PSf-based membrane shows the highest activation energy while PEI-based membrane the lowest. These results can be interpreted according to the heat of salt sorption, $\Delta H_s$, from the aqueous solution to the membrane phase and the activation energy of salt diffusion $E_D$ in the membrane, and the sum of which is the activation energy of salt passage $E_p$. While $\Delta H_s$ is usually negative (due to exothermic salt sorption) [37], $E_D$ is positive and the sign of the $E_p$ depends on the relative importance of $\Delta H_s$ and $E_D$. When ionic sorption becomes dominant, $E_p$ becomes negative; however, $E_p$ turns to positive when diffusion becomes dominant.

As mentioned earlier, the active polyamide layer of PSf-based TFC membrane is more like a cross-linking structure compared to those of PEI- and PES-based TFC membrane. Hence, it can be expected a large contribution of $E_D$ for the PSf-based TFC membrane in comparison to larger contribution of $\Delta H_s$ (coupled with less $E_D$ contribution) for the PEI-based TFC membrane. Because of this, the sign of $E_p$ turns from positive as shown in PSf-based membrane to negative as shown in PEI-based membrane. For the PES-based membrane, it can be considered to behave more like PEI-based membrane since the polyamide layer of both membranes is more linear structure as evidenced from XPS results.

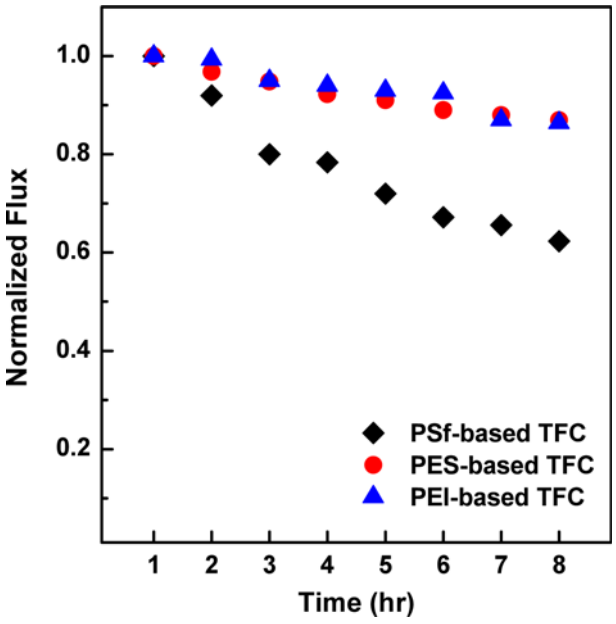


**Fig. 7. Normalized fluxes of TFC NF membranes as a function of time.**

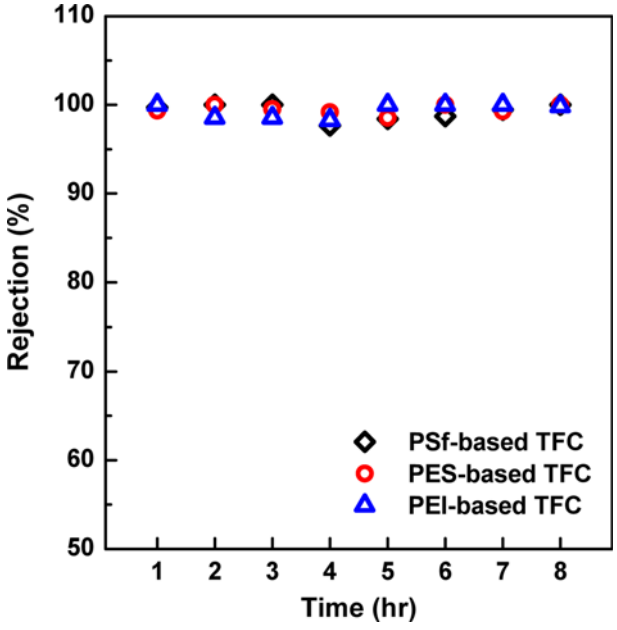


**Fig. 8. BSA rejections of TFC NF membranes as a function of time.**

Besides, the property of substrate membrane is also considered to be an additional factor of the decline in salt rejection. Since the glass transition temperature ($T_g$) of the PSf substrate is the lowest among the prepared substrates, it is expected that the pores of the PSf substrate tend to enlarge more significantly at high operating temperature. This is more likely to cause the poly(piperazine-amide) layer to stretch, leading to an increased pore size of the polyamide layer as reported in previous works [14,36]. The increase in TFC membrane pore size would therefore result in higher flux but lower rejection as evidenced in this work.

2-3. Fouling Properties

Fig. 7 shows the changes in the normalized flux of the prepared TFC membranes over an operation time of 8 hr. The initial flux of PSf-based membrane decreases dramatically by 37.7%, following the PEI- (13.6%) and PES-based TFC membrane (13.0%) for the entire experimental period. Considering that the PSf-based TFC membrane has the lowest contact angle (see Fig. 1) and roughest top surface (see Fig. 2) among the three studied membranes, there is reason to believe that these two factors contribute greatly to the severe flux decline in PSf-based membrane. The significant flux decline is likely due to the fouling problem caused by the accumulation of BSA foulant in the valleys of the rough membrane surface, resulting in "valley clogging" as elucidated in other research work [38]. The similarity of the surface roughness for the PEI- and PES-based membrane has made both membranes to have very similar normalized flux results. With respect to BSA rejection data as shown in Fig. 8, all the resultant membranes are able to exhibit almost complete rejection of BSA foulants, regardless of substrate material used. This excellent separation efficiency can be attributed to the small surface pore size of the TFC NF membranes in comparison to the size of BSA macromolecules [31,39]. Note that small dye molecules could also be used to study membrane fouling as reported elsewhere [40,41], but the incomplete removal of small dye molecules by NF membrane might cause the molecules to trap within membrane structure/matrix, affecting fouling analysis.

## CONCLUSIONS

Poly(piperazineamide) thin selective layer was successfully formed over the top surface of substrate made from different polymers. All the prepared TFC membranes were characterized using FESEM, AFM and XPS before being evaluated under various operating conditions. Based on the experimental data obtained, it can be concluded that:

(a) Permeate flux for all the studied TFC membranes decreases with an increase in solute ($Na_2SO_4$) concentration. Solute separation rate is also found to decrease at higher solute concentration, which can be explained by the Donnan equilibrium theory.

(b) The thermal stability of the TFC membranes is found to be influenced by the materials used for substrate making. Depending on the polymeric materials used for TFC substrate, the performance of composite NF membrane could vary as a function of temperature. Of the three TFC membranes studied, the PEI-based membrane was able to achieve the highest flux and rejection with increasing temperature.

(c) The fouling property of composite NF membrane is most likely governed by the surface roughness and hydrophilicity of the poly(piperazine-amide) layer in which the membrane (PSf-based membrane) with the roughest surface and lowest hydrophilicity tends to have more significant water flux decline. It is because BSA foulants tend to accumulate more easily on the rougher surface than that of smoother surface.

Overall, it can be confirmed that the use of different polymeric substrate would have impacts on not only the physico-chemical properties of the composite NF membranes but also separation performance. As evidenced in this work, the three TFC membranes

made of different polymeric substrates demonstrated different results when the membranes were subjected to different feed concentration and operating temperature, even though the PA layer of all of them was made of same active monomers. Considering the stability of membrane at relatively high operating temperature and antifouling property, it can be said that the TFC membrane made of PEI substrate outperforms the TFC membrane made of PSf and PES substrate.

## ACKNOWLEDGEMENTS

The authors are grateful for research financial support by the Ministry of Education under Long-term Research Grant Scheme (Vot no. 4L803). Author, N. Misdan thanks the sponsorship given by the Ministry of Education under MyBrain15 (MyPhD) scheme during her Ph.D. studies. Thanks also given to Dr. Dipak Rana from University of Ottawa (Canada) for the XPS characterization.

## REFERENCES

1. S. H. Chen, D. J. Chang, R. M. Liou, C. S. Hsu and S. S. Lin, *J. Appl. Polym. Sci.*, **83**, 1112 (2002).
2. W. J. Lau, A. F. Ismail, P. S. Goh, N. Hilal and B. S. Ooi, *Sep. Purif. Rev.*, DOI:10.1080/15422119.2014.882355.
3. P. Eriksson, *Environ. Prog.,* **7**, 58 (1988).
4. F. Liu, G. Zhang, Q. Meng and H. Zhang, *Chin. J. Chem. Eng.*, **16**, 441 (2008).
5. A. Rahimpour, M. Jahanshahi, N. Mortazavian, S. S. Madaeni and Y. Mansourpanah, *Appl. Surf. Sci.*, **256**, 1657 (2010).
6. D. Hu, Z. L. Xu and C. Chen, *Desalination*, **301**, 75 (2012).
7. A. L. Ahmad, B. S. Ooi, A. Wahab Mohammad and J. P. Choudhury, *J. Appl. Polym. Sci.*, **94**, 394 (2004).
8. J. Jegal, S. G. Min and K. H. Lee, *J. Appl. Polym. Sci.*, **86**, 2781 (2002).
9. M. Namvar-Mahboub and M. Pakizeh, *Korean J. Chem. Eng.*, **31**, 327 (2014).
10. W. J. Lau, A. F. Ismail, N. Misdan and M. A. Kassim, *Desalination*, **287**, 190 (2012).
11. L. Hu, S. Zhang, R. Han and X. Jian, *Appl. Surf. Sci.*, **258**, 9047 (2012).
12. N. Misdan, W. J. Lau and A. F. Ismail, *Desalination*, **287**, 228 (2012).
13. D. Li and H. Wang, *J. Mater. Chem.*, **20**, 4551 (2010).
14. J. Wei, X. Jian, C. Wu, S. Zhang and C. Yan, *J. Membr. Sci.*, **256**, 116 (2005).
15. E. S. Kim, Y. J. Kim, Q. Yu and B. Deng, *J. Membr. Sci.*, **344**, 71 (2009).
16. H. I. Kim and S. S. Kim, *J. Membr. Sci.*, **286**, 193 (2006).
17. S. Verissimo, K. V. Peinemann and J. Bordado, *J. Membr. Sci.*, **279**, 266 (2006).
18. M. Namvar-Mahboub and M. Pakizeh, *Sep. Purif. Technol.*, **119**, 35 (2013).
19. C. R. Wu, S. H. Zhang, D. L. Yang, J. Wei, C. Yan and X. G. Jian, *J. Membr. Sci.*, **279**, 238 (2006).
20. R. Han, S. Zhang, L. Hu, S. Guan and X. Jian, *J. Membr. Sci.*, **370**, 91 (2011).
21. N. Fujiwara and H. Matsuyama, *Desalination*, **227**, 295 (2008).
22. O. Kedem and A. Katchalsky, *Trans Faraday Soc.*, **59**, 1918 (1963).
23. M. Pontie, H. Buisson, C. K. Diawara and H. Essis-Tome, *Desalination*, **157**, 127 (2003).
24. A. M. Hidalgo, G. Leon, M. Gomez, M. D. Murcia, E. Gomez and J. L. Gomez, *Desalination*, **315**, 70 (2013).
25. K. S. Spiegler and O. Kedem, *Desalination*, **1**, 311 (1966).
26. J. Schaep, B. Van der Bruggen, C. Vandecasteele and D. Wilms, *Sep. Purif. Technol.*, **14**, 155 (1998).
27. G. M. Geise, H. B. Park, A. C. Sagle, B. D. Freeman and J. E. McGrath, *J. Membr. Sci.*, **369**, 130 (2011).
28. H. K. Lonsdale, U. Merten and R. L. Riley, *J. Appl. Polym. Sci.*, **9**, 1341 (1965).
29. D. R. Paul, *J. Membr. Sci.*, **241**, 371 (2004).
30. T. Matsuura, *Synthetic Membranes and Membrane Separation Processes*, CRC Press (1993).
31. N. Misdan, W. J. Lau, A. F. Ismail, T. Matsuura and D. Rana, *Desalination*, **344**, 198 (2014).
32. W. J. Lau and A. F. Ismail, *Desalination*, **245**, 198 (2009).
33. C. S. Ong, W. J. Lau and A. F. Ismail, *Desalin. Water Treat.,* **50**, 245 (2012).
34. A. F. Ismail and W. J. Lau, *Desalin. Water Treat.*, **6**, 281 (2009).
35. H. Mehdizadeh, J. M. Dickson and P. K. Eriksson, *Ind. Eng. Chem. Res.*, **28**, 814 (1989).
36. R. R. Sharma and S. Chellam, *Environ. Sci. Technol.*, **39**, 5022 (2005).
37. K. Kulisa, *Chem. Anal.*, **49**, 665 (2004).
38. E. M. Vrijenhoek, S. Hong and M. Elimelech, *J. Membr. Sci.*, **188**, 115 (2001).
39. N. Misdan, W. J. Lau, A. F. Ismail and T. Matsuura, *Desalination*, **329**, 9 (2013).
40. C. Z. Liang, S. P. Sun, F. Y. Li, Y. K. Ong and T. S. Chung, *J. Membr. Sci.*, **469**, 306 (2014).
41. Y. K. Ong, F. Y. Li, S. P. Sun, B. W. Zhao, C. Z. Liang and T. S. Chung, *Chem. Eng. Sci.*, **114**, 51 (2014).